ELSEVIER

Journal of Chromatography A, 724 (1996) 13–25

JOURNAL OF CHROMATOGRAPHY A

Modelling and analysis of the elution stage of "perfusion chromatography" Effects of intraparticle convective velocity and microsphere size on system performance

Y. Xu, A.I. Liapis*

Department of Chemical Engineering and Biochemical Processing Institute, University of Missouri–Rolla, Rolla, MO 65401-0249, USA

First received 18 April 1995; revised manuscript received 17 July 1995

Abstract

A mathematical model describing the dynamic elution (elution stage) in columns with spherical bidisperse perfusive or spherical bidisperse purely diffusive adsorbent particles is presented and its solution is obtained numerically. The desorption of bovine serum albumin (BSA) from spherical anion-exchange porous particles was studied for different values of the intraparticle Peclet numbers of the adsorbate, $(Pe_{intra})_a$, and eluent, $(Pe_{intra})_e$, and of the microsphere diameter, d_m. It was found that as $(Pe_{intra})_a$ increases, the asymmetry of the elution peak of the adsorbate (at the exit of the column) decreases, the peak height increases and the time, T_e, required for the elution of the adsorbate decreases. The results also show that T_e decreases, and the average bulk concentration of the adsorbate, $C_{d,bulk}$, in the solution collected at the exit of the column and the concentration factor, CF, increase as the diameter of the microsphere, d_m, decreases and the value of $(Pe_{intra})_a$ increases for the adsorbent particles used in the column. Furthermore, the results clearly show that for given values of d_m and $(Pe_{intra})_a$, the systems with reverse flow during the elution stage exhibit better performance than that obtained from the system where the eluent flows in the same direction in the column during the elution stage as was the direction of flow of the adsorbate in the column during the adsorption stage.

Keywords: Perfusion chromatography; Thermodynamic parameters; Stationary phases, LC; Mathematical modelling; Albumin

1. Introduction

The modelling and analysis of the elution stage of affinity adsorption separations in fixed beds with purely diffusive adsorbent particles has been studied by Arve and Liapis [1] and Liapis [2]. While the adsorption stage of "perfusion chromatography" has been and is being studied quantitatively through the construction and solution of mathematical models [3–9] that describe the dynamic behavior of the adsorption stage of affinity adsorption separations in fixed beds with

* Corresponding author.

0021-9673/96/$15.00
SSDI 0021-9673(95)00952-3

perfusive adsorbent particles, there have been, to our knowledge, no comparable quantitative studies reported in the literature on the modelling and analysis of the elution stage of "perfusion chromatography". In this work, as in previous publications [3–9], we define "perfusion chromatography" to refer to any chromatographic system in which the intraparticle velocity, v_p, is non-zero [3–10].

Liapis and McCoy [5], Liapis et al. [8] and Heeter and Liapis [9] have considered that the perfusive adsorbent particles with a bidisperse [5,8,9] porous structure have a macroporous region [3,5,6,8–10] in which intraparticle convection and pore diffusion occur, and a microporous [5,8,9] region made up of spherical microparticles (microspheres [5,8–10]) that are taken to be purely diffusive. In this work, the adsorption and elution stages of the system involving the adsorption of bovine serum albumin (BSA) into spherical anion-exchange porous particles packed in a column were studied. The dynamic behavior of the adsorption stage was studied quantitatively through the use of the mathematical model developed by Liapis et al. [8], while the dynamic behavior of the elution stage was quantified through the solution of a mathematical model developed and presented in this work.

2. Mathematical model of the elution stage of "perfusion chromatography"

At the beginning of the elution stage in a fixed bed, it is considered that the adsorbate molecules have been adsorbed on active sites immobilized on the internal surface of the porous adsorbent particles. It is also considered that the concentrations of the contaminants have been reduced to a specified low level during the wash stage [1,2,7,11,12]. The eluting agent is taken to be a non-selective eluent that is considered not to be adsorbed biospecifically or non-specifically, and is introduced into the column through the feed solution. Elution is considered to take place into a flowing liquid stream in a fixed bed of spherical perfusive adsorbent particles of bidisperse porous structure under isothermal conditions. The differential mass balance expressions for the adsorbate and the eluent in the flowing fluid stream are given by the equations

$$\frac{\partial C_d}{\partial t_e} - D_L \cdot \frac{\partial^2 C_d}{\partial x^2} + \frac{V_f}{\varepsilon} \cdot \frac{\partial C_d}{\partial x} = -\frac{(1-\varepsilon)}{\varepsilon} \cdot \frac{\partial \bar{C}_{ps}}{\partial t_e} \tag{1}$$

$$\frac{\partial C_{de}}{\partial t_e} - D_{Le} \cdot \frac{\partial^2 C_{de}}{\partial x^2} + \frac{V_f}{\varepsilon} \cdot \frac{\partial C_{de}}{\partial x} = -\frac{(1-\varepsilon)}{\varepsilon} \cdot \frac{\partial \bar{C}_{pe}}{\partial t_e} \tag{2}$$

The initial and boundary conditions of Eqs. 1 and 2 are as follows:

$$\text{at } t_e = 0, \quad C_d = \psi(x), 0 \leq x \leq L \tag{3}$$

$$\text{at } t_e = 0, \quad C_{de} = 0, 0 \leq x \leq L \tag{4}$$

$$\text{at } x = 0, \quad \frac{V_f}{\varepsilon} \cdot C_d\Big|_{x=0} - D_L \frac{\partial C_d}{\partial x}\Big|_{x=0} = 0, \quad t_e > 0 \tag{5}$$

$$\text{at } x = 0, \quad \frac{V_f}{\varepsilon} \cdot C_{de}\Big|_{x=0} - D_{Le} \frac{\partial C_{de}}{\partial x}\Big|_{x=0} = \frac{V_f}{\varepsilon} C_{de,in}, t_e > 0 \tag{6}$$

$$\text{at } x = L, \quad \frac{\partial C_d}{\partial x}\Big|_{x=L} = 0, t_e > 0 \tag{7}$$

$$\text{at } x = L, \quad \frac{\partial C_{de}}{\partial x}\Big|_{x=L} = 0, t_e > 0 \tag{8}$$

The value of $C_{de,in}$ may be constant or it may vary with time. Expressions for estimating D_L and D_{Le} have been presented by Arnold et al. [13] and Gunn [14,15], but in certain systems the axial dispersion is so low that by setting its value equal to zero the error introduced in the prediction of the behavior of an affinity adsorption system is not significant [13,16]. The expression of the function $\psi(x)$ in Eq. 3 is determined from the values of C_d along x obtained at the end of the adsorption stage [8,9] if there were no contaminants, or from the values of C_d along x obtained at the end of the wash stage if there were contaminants [2].

The spherical perfusion adsorbent particles with a bidisperse [5,8,9,17] porous structure are considered to have a microporous [5,8,9,17] re-

gion made by spherical microparticles (microspheres [5,8–10,17]) that are taken to be purely diffusive, and a macroporous [5,8,9,17] region made by the macropores [3,5–10] in which intraparticle convection and pore diffusion occur; it should be noted here that the model of Liapis et al. [8] is not limited by the significant restrictions of the model of Carta and Rodrigues [17]. In Fig. 1 of Ref. [8], a diagram of the spherical perfusive adsorbent particle with a bidisperse porous structure is shown.

The differential mass balances for the adsorbate and the eluent in the macroporous region of a perfusive adsorbent particle of spherical geometry are given by

$$\varepsilon_p \cdot \frac{\partial C_p}{\partial t_e} + \varepsilon_p v_{pR} \cdot \frac{\partial C_p}{\partial R} + \varepsilon_p v_{p\theta}\left(\frac{1}{R}\right)\frac{\partial C_p}{\partial \theta} + (1-\varepsilon_p)\frac{\partial \bar{C}_s}{\partial t_e} = \varepsilon_p D_p\left[\left(\frac{1}{R^2}\right)\frac{\partial}{\partial R}\left(R^2 \cdot \frac{\partial C_p}{\partial R}\right) + \left(\frac{1}{R^2 \sin\theta}\right)\frac{\partial}{\partial \theta}\left(\sin\theta \frac{\partial C_p}{\partial \theta}\right)\right] \quad (9)$$

$$\varepsilon_p \cdot \frac{\partial C_{pe}}{\partial t_e} + \varepsilon_p v_{pR} \cdot \frac{\partial C_{pe}}{\partial R} + \varepsilon_p v_{p\theta}\left(\frac{1}{R}\right)\frac{\partial C_{pe}}{\partial \theta} + (1-\varepsilon_p)\frac{\partial \bar{C}_{pme}}{\partial t_e} = \varepsilon_p D_{pe}\left[\left(\frac{1}{R^2}\right)\frac{\partial}{\partial R}\left(R^2 \cdot \frac{\partial C_{pe}}{\partial R}\right) + \left(\frac{1}{R^2 \sin\theta}\right)\frac{\partial}{\partial \theta}\left(\sin\theta \frac{\partial C_{pe}}{\partial \theta}\right)\right] \quad (10)$$

The variables v_{pR} and $v_{p\theta}$ represent the intraparticle velocity components along the R and θ directions, respectively. The expressions for v_{pR} and $v_{p\theta}$ are given by Eqs. 7 and 8 of Ref. [8] and were obtained from the analytical expressions for the stream functions developed by Neale et al. [18]. It has been found [8,19] from numerous parametric calculations that for various adsorption systems the value of H in Eqs. 7 and 8 of ref. [8] is essentially equal to zero; the value of H for the system considered in this work is approximately equal to zero. When H is taken to be approximately equal to zero ($H \approx 0$) in Eqs. 7 and 8 of Ref. [8], the expressions for v_{pR} and $v_{p\theta}$ take the forms given by Eqs. 37 and 38 of Ref. [8] and the intraparticle Peclet numbers for the adsorbate, $(Pe_{intra})_a$, and the eluent, $(Pe_{intra})_e$, are then defined by Eqs. 11 and 12, respectively:

$$(Pe_{intra})_a = \frac{(FV_f)d_p}{D_p} \quad (11)$$

$$(Pe_{intra})_e = \frac{(FV_f)d_p}{D_{pe}} \quad (12)$$

The value of F can be calculated from Eq. 10 of Ref. [8]. It should be noted that since the values of D_p and D_{pe} are different, then the values of $(Pe_{intra})_a$ and $(Pe_{intra})_e$ will also be different.

The initial and boundary conditions of Eqs. 9 and 10 are as follows:

$$\text{at } t_e = 0, \quad C_p = \gamma(R,\theta), \ 0 \le R \le R_p, \ 0 \le \theta \le \pi \quad (13)$$

$$\text{at } t_e = 0, \quad C_{pe} = 0, \ 0 \le R \le R_p, \ 0 \le \theta \le \pi \quad (14)$$

$$\text{at } R = R_p, \ C_p = C_d, \ 0 \le \theta \le \pi, \ t_e > 0 \quad (15)$$

$$\text{at } R = R_p, \ C_{pe} = C_{de}, \ 0 \le \theta \le \pi, \ t_e > 0 \quad (16)$$

$$\text{at } R = 0, \quad C_p = \text{finite}, \ 0 \le \theta \le \pi, \ t_e > 0 \quad (17)$$

$$\text{at } R = 0, \quad C_{pe} = \text{finite}, \ 0 \le \theta \le \pi, \ t_e > 0 \quad (18)$$

$$\text{at } \theta = 0, \quad \left.\frac{\partial C_p}{\partial \theta}\right|_{\theta=0} = 0, \ 0 \le R \le R_p, \ t_e > 0 \quad (19)$$

$$\text{at } \theta = 0, \quad \left.\frac{\partial C_{pe}}{\partial \theta}\right|_{\theta=0} = 0, \ 0 \le R \le R_p, \ t_e > 0 \quad (20)$$

$$\text{at } \theta = \pi, \quad \left.\frac{\partial C_p}{\partial \theta}\right|_{\theta=\pi} = 0, \ 0 \le R \le R_p, \ t_e > 0 \quad (21)$$

$$\text{at } \theta = \pi, \quad \left.\frac{\partial C_{pe}}{\partial \theta}\right|_{\theta=\pi} = 0, \; 0 \leq R \leq R_p, \; t_e > 0 \tag{22}$$

The differential mass balances for the adsorbate and the eluent in a purely diffusive spherical microparticle (microsphere) are given by

$$\varepsilon_{pm} \cdot \frac{\partial C_{pm}}{\partial t_e} + \left(\frac{1}{1-\varepsilon_p}\right)\frac{\partial C_{sm}}{\partial t_e} = \varepsilon_{pm} D_{pm}\left(\frac{\partial^2 C_{pm}}{\partial r^2} + \frac{2}{r}\cdot\frac{\partial C_{pm}}{\partial r}\right) \tag{23}$$

$$\varepsilon_{pm} \cdot \frac{\partial C_{pme}}{\partial t_e} = \varepsilon_{pm} D_{pme}\left(\frac{\partial^2 C_{pme}}{\partial r^2} + \frac{2}{r}\cdot\frac{\partial C_{pme}}{\partial r}\right) \tag{24}$$

The functional form of the accumulation term $\partial C_{sm}/\partial t_e$ in Eq. 23 depends, for a given position r in the microsphere, on the concentration of the eluent at the given position. In this work, the following two cases are considered:

(a) If for a given r the concentration of the eluent, C_{pme}, is less than the critical eluent concentration, $C_{pme,cr}$ (the critical eluent concentration, $C_{pme,cr}$, is considered to represent the minimum concentration of the eluent that could induce desorption of adsorbate), then

$$\frac{\partial C_{sm}}{\partial t_e} = k_1 C_{pm}(C_T - C_{sm}) - k_2 C_{sm} \tag{25}$$

(b) If for a given r the concentration of the eluent, C_{pme}, is greater than or equal to the critical concentration, $C_{pme,cr}$, then

$$\frac{\partial C_{sm}}{\partial t_e} = -k_3 C_{sm} \tag{26}$$

Functional forms other than those used in the right-hand sides of Eqs. 25 and 26 could be used, depending on the mechanism of adsorption for case (a) and on the mechanism of desorption for case (b). It should be noted that case (a) implies that there could be adsorption of adsorbate as long as $C_{pme} < C_{pme,cr}$, while case (b) indicates that there is desorption of adsorbate as long as $C_{pme} \geq C_{pme,cr}$. In this work, when case (a) occurs then the term $\partial C_{sm}/\partial t_e$ in Eq. 23 is replaced by the right-hand side of Eq. 25; when case (b) occurs then the term $\partial C_{sm}/\partial t$ in Eq. 23 is replaced by the right-hand side of Eq. 26.

The initial and boundary conditions of Eqs. 23–26 are as follows:

$$\text{at } t_e = 0, \quad C_{pm} = \delta(r), \; 0 \leq r \leq r_m \tag{27}$$

$$\text{at } t_e = 0, \quad C_{sm} = \phi(r), \; 0 \leq r \leq r_m \tag{28}$$

$$\text{at } r = 0, \quad \frac{\partial C_{pm}}{\partial r} = 0, \; t_e > 0 \tag{29}$$

$$\text{at } r = 0, \quad \frac{\partial C_{pme}}{\partial r} = 0, \; t_e > 0 \tag{30}$$

$$\text{at } r = r_m, \quad C_{pm} = C_p(t, R, \theta), \; t_e > 0 \tag{31}$$

$$\text{at } r = r_m, \quad C_{pme} = C_{pe}(t, R, \theta), \; t_e > 0 \tag{32}$$

The expressions of the functions $\gamma(R, \theta)$, $\delta(r)$ and $\phi(r)$ in Eqs. 13, 27 and 28 are determined from the values of C_p along R and θ, and the values of C_{pm} and C_{sm} along r obtained at the end of the adsorption stage [8,9] if there were no contaminants, or from the values of C_p along R and θ, and the values of C_{pm} and C_{sm} along r obtained at the end of the wash stage if there were contaminants [2].

The expressions for the accumulation terms $\partial \bar{C}_{ps}/\partial_{te}$, $\partial \bar{C}_{pe}/\partial t_e$, $\partial \bar{C}_s/\partial t_e$ and $\partial \bar{C}_{pme}/\partial t_e$ in Eqs. 1, 2, 9 and 10, respectively, are given in Ref. [19]. For a given pair of values of R and θ, the average concentration of the adsorbate in the adsorbed phase, $\bar{C}_{sa}$, is obtained from the following expression:

$$\bar{C}_{sa} = (1-\varepsilon_p)\frac{3}{r_m^3}\left[\int_0^{r_m}\left(\frac{1}{1-\varepsilon_p}\right)C_{sm} r^2 \, dr\right] \tag{33}$$

The dynamic behavior of the adsorption stage of a column adsorption system involving spherical perfusive adsorbent particles with a bidisperse porous structure is obtained by solving simultaneously Eqs. 1, 6, 24 and 25 of Ref. [8], while the dynamic behavior of the elution stage is obtained from the simultaneous solution of Eqs. 1, 2, 9, 10, 23, 24, 25 and 26 in this work.

Table 1
Values of the parameters of the adsorption stage of the column system involving the adsorption of BSA into spherical anion-exchange porous adsorbent particles

$C_{d,in}$0.1 kg/m^3,	$D_{pm} = 7.375 \cdot 10^{-12}$ m^2/s,
$C_T = 78.3$ kg/m^3,	$D_L = 0$,
$d_p = 1.5 \cdot 10^{-5}$ m,	$K = k_1/k_2 = 8.026$ m^3/kg,
$\varepsilon = 0.35$,	$k_1 = 1.05$ m^3/kg·s,
$\varepsilon_p = 0.45$,	$k_2 = 0.131$ s^{-1},
$\varepsilon_{pm} = 0.50$,	$L = 0.1$ m,
$T = 296$ K,	$V_f = 2.778 \cdot 10^{-3}$ m/s
$D_p = 13.275 \cdot 10^{-12}$ m^2/s,	

2.1. Numerical solution

The solution of the equations that describe the dynamic behavior of the adsorption and elution stages was obtained by using the numerical method presented in Refs. [8] and [19].

3. Results and discussion

In this work, the diameter of the adsorbent particles, d_p, is taken to be $1.5 \cdot 10^{-5}$ m, while three different values for the diameter of the micoroparticles, d_m, were employed in the studies in this work: $d_m =$ (a) $7.00 \cdot 10^{-8}$, (b) $7.00 \cdot 10^{-7}$ and (c) $7.00 \cdot 10^{-6}$ m. In Tables 1 and 2, the values of the parameters used for the dynamic simulations of the adsorption and elution stages of the adsorption system studied in this work are presented. The values of other parameters are reported in the captions of the figures. The eluent's effective pore diffusivities in the macroporous and microporous regions of the adsorbent particles are about 21 times larger than the corresponding effective pore diffusivities of the adsorbate (BSA) molecules, as can be observed from the data in Table 2.

Table 2
Values of the parameters of the elution stage of the column system involving the desorption of BSA from spherical anion-exchange porous adsorbent particles

$C_{d,in} = 0$,	$D_{pe} = 2.79 \cdot 10^{-10}$ m^2/s,
$C_{de,in} = 6.0$ kg/m^3,	$D_{pme} = 1.55 \cdot 10^{-10}$ m^2/s,
$C_{pme,cr} = 0.75 C_{de,in}$,	$D_L = 0$,
$C_T = 78.3$ kg/m^3,	$D_{Le} = 0$,
$d_p = 1.5 \cdot 10^{-5}$ m,	$K = k_1/k_2 = 8.026$ m^3/kg,
$\varepsilon = 0.35$,	$k_1 = 1.05$ m^3/kg·s,
$\varepsilon_p = 0.45$,	$k_2 = 0.131$ s^{-1},
$\varepsilon_{pm} = 0.50$,	$k_3 = 106.2$ s^{-1},
$T = 296$ K,	$L = 0.1$ m,
$D_p = 13.275 \cdot 10^{-12}$ m^2/s,	$V_f = 2.778 \cdot 10^{-3}$ m/s
$D_{pm} = 7.375 \cdot 10^{-12}$ m^2/s,	

The dynamic percentage utilization of the adsorptive capacity of the column at 1% breakthrough during the adsorption stage, is presented for different values of d_m and $(Pe_{intra})_a$ in Table 3; in this work, the adsorption stage is terminated at 1% breakthrough and then the elution stage starts. The total adsorptive capacity of the column is defined as the total amount of adsorbate in the adsorbed phase (in the column) at equilib-

Table 3
Adsorption stage: dynamic percentage utilization of the adsorptive capacity of the column at 1% $\{[C_d(t, L)/C_{d,in}] \cdot 100 = 1\%\}$ breakthrough

d_m (m)	$(Pe_{intra})_a$ [a]	Time at which 1% breakthrough occurs (min)	Dynamic percentage utilization at 1% breakthrough
$7.00 \cdot 10^{-8}$	0	108.00	79.151
	1	108.00	79.151
	2	108.40	79.468
	5	109.00	79.909
	10	111.00	81.377
	20	116.00	85.047
	30	119.60	87.695
$7.00 \cdot 10^{-7}$	0	107.80	79.029
	1	107.80	79.030
	2	108.00	79.176
	5	108.80	79.762
	10	110.80	81.230
	20	115.60	84.754
	30	119.40	87.547
$7.00 \cdot 10^{-6}$	0	88.80	65.069
	1	88.80	65.069
	2	88.90	65.143
	5	89.60	65.656
	10	91.80	67.270
	20	96.60	70.794
	30	100.26	73.483

For all calculations $d_p = 1.5 \cdot 10^{-5}$ m.
[a] See Eq. 11.

rium (evaluated with respect to the value of $C_{d,in}$). The dynamic utilization of the adsorptive capacity of the column is defined as the ratio of the total amount of adsorbate in the adsorbed phase of the column when the desired breakthrough occurs to the total adsorptive capacity of the column. The results in Table 3 show that for a given value of d_m, the dynamic percentage utilization of the adsorptive capacity of the column increases as the value of $(Pe_{intra})_a$ increases. Furthermore, the results in Table 3 suggest that decreases in dynamic percentage utilization with increasing values of d_m could be reduced by increasing values of $(Pe_{intra})_a$. Thus, the simulation results in Table 3 indicate that the amount of BSA in the adsorbed phase increases during the adsorption stage, as the value of d_m decreases and the value of $(Pe_{intra})_a$ increases [8,9] for the adsorbent particles used in the column.

In this work, the dynamic performance of the elution stage was studied under the following two directions of the flowing fluid stream of the eluent: (I) the eluent flows in the same direction in the column during the elution stage as was the direction of flow of the adsorbate in the column during the adsorption stage, and (II) the direction of flow of the eluent in the column during the elution stage is reverse to the direction of flow of the adsorbate in the column during the adsorption stage. In Figs. 1–3, the dimensionless exiting concentrations of the adsorbate, $C_d(t_e, L)/C_{d,in}$, during the elution stage, are presented, for cases I and II and for three different values of $(Pe_{intra})_a$; the value of $C_{d,in}$ in Figs. 1–3 is equal to 0.1 kg/m^3. The results in Figs. 1–3 indicate that as the value of the intraparticle Peclet number, $(Pe_{intra})_a$, of the adsorbate increases, the asymmetry of the elution peak of the adsorbate decreases, the peak height increases and the time required for the elution of the adsorbate decreases. Also, the results in Figs. 1–3 indicate that when reversed flow is employed (case II), for a given value of $(Pe_{intra})_a$, the peak height is larger and the time required for the elution of the adsorbate is smaller than the peak height and elution time obtained from case I; furthermore, the results in

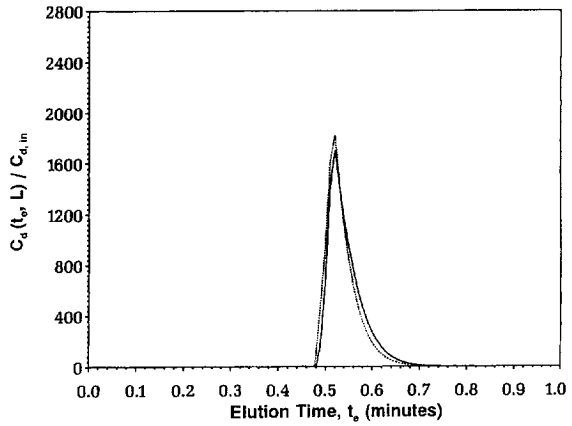

Fig. 1. Dimensionless concentration of adsorbate in the effluent stream versus elution time, when $(Pe_{intra})_a = (Pe_{intra})_e = 0$ and $d_m = 7.00 \cdot 10^{-7}$ m. Full line = case I; broken line = case II.

Figs. 1–3 indicate that the effects of reverse flow decrease as the intraparticle Peclet number, $(Pe_{intra})_a$, of the adsorbate increases. In Table 4, the duration of the elution stage, T_e, the average bulk concentration of the adsorbate, $C_{d,bulk}$, in the fluid collected at the exit of the column during the elution stage, and the concentration factor, CF, are presented for cases I and II and for different values of d_m and $(Pe_{intra})_a$. $C_{d,bulk}$ and CF were obtained from the following expressions:

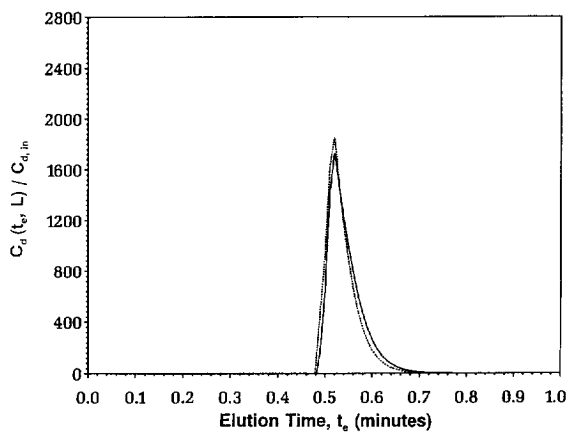

Fig. 2. Dimensionless concentration of adsorbate in the effluent stream versus elution time, when $(Pe_{intra})_a = 5$, $(Pe_{intra})_e = 0.238$ and $d_m = 7.00 \cdot 10^{-7}$m. Full line = case I; broken line = case II.

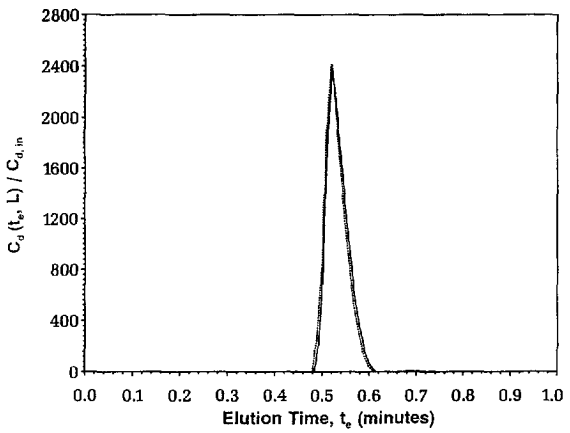

Fig. 3. Dimensionless concentration of adsorbate in the effluent stream versus elution time, when $(Pe_{intra})_a = 30$, $(Pe_{intra})_e = 1.427$ and $d_m = 7.00 \cdot 10^{-7}$ m. Full line = case I; broken line–case II.

$$C_{d,bulk} = \frac{1}{T_e}\left(\int_0^{T_e} C_d(t_e, L)\, dt_e\right) \quad (34)$$

$$CF = \frac{C_{d,bulk}}{C_{d,in}} \quad (35)$$

where T_e represents the total time of the duration of the elution stage and $C_{d,in}$ is the inlet concentration of the adsorbate during the adsorption stage ($C_{d,in} = 0.1$ kg/m^3 in this work). It was arbitrarily selected, in this work, to terminate the elution stage [after the time at which the maximum of $C_d(t_e, L)$ was encountered] when the concentration of the adsorbate in the effluent stream has decreased to 0.5% of the inlet concentration of the adsorbate in the adsorption stage. The concentration factor, CF, may be seen to represent the overall concentrating effect of the adsorption and elution stages on the adsorbate. The higher the amount of adsorbate adsorbed during the adsorption stage and the shorter the total time of the duration of the elution stage, T_e, the higher will be the value of the concentration factor, CF. The results in Table 4 indicate that T_e decreases and $C_{d,bulk}$ and CF increase as the diameter of the microsphere, d_m, decreases and the value of $(Pe_{intra})_a$ increases for the adsorbent particles used in the column. The significant change in the results occurs as d_m increases from $7.00 \cdot 10^{-8}$ to $7.00 \cdot 10^{-6}$ m. It is also observed in Table 4 that for a given value of d_m, the differences in the values of T_e, $C_{d,bulk}$ and CF are not significant when $0 \leqslant (Pe_{intra})_a \leqslant 5$. Furthermore, the results in Table 4 clearly show that for given values of d_m and $(Pe_{intra})_a$, the systems of case II (systems with reverse flow during the elution stage) exhibit better performance (lower values for T_e and higher values for $C_{d,bulk}$ and CF) than that obtained from the systems of case I (same direction of flow during the adsorption and elution stages).

In Fig. 4, the breakthrough curves of the eluent are presented for values of the intraparticle Peclet number of the eluent, $(Pe_{intra})_e$, of 0, 0.048, 0.095, 0.238, 0.476, 0.952 and 1.427; the corresponding values of the intraparticle Peclet number of the adsorbate, $(Pe_{intre})_a$, are 0, 1, 2, 5, 10, 20 and 30. The results in Fig. 4 show that the breakthrough curves of the eluent overlap for all the different values of $(Pe_{intra})_e$ studied in this work, and therefore the results in fig. 4 indicate that the breakthrough behavior of the eluent obtained from a column having purely diffusive ($F = 0$) particles is not significantly different from the breakthrough behavior of the eluent obtained from a column with perfusive ($F > 0$) particles, during the elution stage of the systems examined in this work. While the effect of intraparticle convective flow on the dynamic behavior of the adsorption and elution of the adsorbate could be significant (as can be observed from the results in Table 3 and 4 and Figs. 1–3), the effect of intraparticle convective flow on the dynamic behavior of the eluent, for the systems studied in this work, is not significant because (a) the effective pore diffusivities of the eluent, D_{pe} and D_{pme}, are 21 times larger than those of the adsorbate, (b) the eluent does not interact with the surface of the pores of the adsorbent particles and (c) the inlet concentration of the eluent is high enough that together with the large values of the effective pore diffusivities of the eluent provide large mass fluxes for the eluent in the macroporous and microporous regions of the adsorbent particles.

In Figs. 5 and 6, the dimensionless isoconcentration profiles of the adsorbate and eluent in the

Table 4
Duration of the elution stage, T_e, average bulk concentration of adsorbate, $C_{d,bulk}$, in the fluid collected at the exit of the column during the elution stage and concentration factor, CF ($CF = C_{d,bulk}/C_{d,in}$), for cases I and II and for different values of d_m and $(Pe_{intra})_a$

d_m (m)	$(Pe_{intra})_a$ [a]	Case I			Case II		
		Duration of elution stage, T_e (min)	Average bulk concentration of adsorbate, $C_{d,bulk}$ (kg/m^3)	CF	Duration of elution stage, T_e (min)	Average bulk concentration of adsorbate, $C_{d,bulk}$ (kg/m^3)	CF
$7.00 \cdot 10^{-8}$	0	0.94	11.484	114.84	0.91	11.863	118.63
	1	0.94	11.484	114.84	0.91	11.863	118.63
	2	0.94	11.526	115.26	0.91	11.906	119.06
	5	0.93	11.736	117.36	0.90	12.127	121.27
	10	0.90	12.328	123.28	0.88	12.608	126.08
	20	0.81	14.315	143.15	0.79	14.678	146.78
	30	0.76	15.733	157.33	0.75	15.942	159.42
$7.00 \cdot 10^{-7}$	0	0.94	11.463	114.63	0.91	11.841	118.41
	1	0.94	11.463	114.63	0.91	11.841	118.41
	2	0.94	11.484	114.84	0.91	11.862	118.62
	5	0.93	11.693	116.93	0.90	12.083	120.83
	10	0.90	12.306	123.06	0.88	12.586	125.86
	20	0.81	14.266	142.66	0.79	14.628	146.28
	30	0.76	15.706	157.06	0.75	15.916	159.16
$7.00 \cdot 10^{-6}$	0	0.96	9.241	92.41	0.91	9.749	97.49
	1	0.96	9.241	92.41	0.91	9.749	97.49
	2	0.95	9.349	93.49	0.91	9.760	97.60
	5	0.94	9.523	95.23	0.90	9.946	99.46
	10	0.92	9.969	99.69	0.88	10.422	104.22
	20	0.88	10.968	109.68	0.82	11.771	117.71
	30	0.79	12.682	126.82	0.77	13.012	130.12

The value of d_p is $1.5 \cdot 10^{-5}$ m and $C_{d,in} = 0.1$ kg/m^3 in Eq. 35.
[a] See Eq. 11.

pore fluid of the pores of the macroporous region and the dimensionless isoconcentration profiles of the adsorbate in the adsorbed phase of the adsorbent particle are presented for $(Pe_{intra})_a = 10$ and $(Pe_{intra})_e = 0.476$ and when case I (Fig. 5) or case II (Fig. 6) is employed in the elution stage. In Figs. 5 and 6, the outermost contours represent the isoconcentrations at the surface ($R = R_p$) of the particle. The data in Fig. 5 were obtained for the position in the column located at $x = 0.2L$ and at time $t_e = 0.1$ min, and those in Fig. 6 were obtained at $x = 0.8L$ and $t_e = 0.4$ min. It should be noted that since the results in Fig. 6 were obtained by employing case II in the elution stage, the position in the column located at $x = 0.8L$ during the elution stage corresponds to position $x = 0.2L$ during the adsorption stage; this means that at the beginning of the elution stage the concentration of the adsorbate in the adsorbed phase of the adsorbent particles located at $x = 0.8L$ is higher, in the system presented in Fig. 6, than the concentration of the adsorbate in the adsorbed phase of the adsorbent particles located at positions $x < 0.8L$. The results in Figs. 5 and 6 indicate that when perfusive adsorbent particles are used, the isoconcentration profiles of the adsorbate and eluent exhibit spherical asymmetry [in Ref. [19] it can be observed that the isoconcentration profiles of the adsorbate and eluent exhibit spherical symmetry when

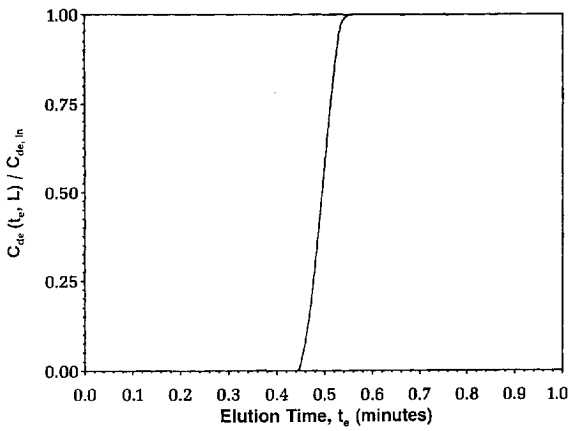

Fig. 4. Breakthrough curves of eluent when $(Pe_{intra})_a = 0$, 1, 2, 5, 10, 20 and 30, $(Pe_{intra})_e = 0$, 0.048, 0.095, 0.238, 0.476, 0.952 and 1.427 and $d_m = 7.00 \cdot 10^{-7}$ m. The breakthrough curves of the eluent overlap for all the different values of $(Pe_{intra})_a$ and $(Pe_{intra})_e$ studied in this work.

$(Pe_{intra})_a = (Pe_{intra})_e = 0$ (purely diffusive adsorbent particles)]. The magnitude of the departure from spherical symmetry of the isoconcentration profiles of the adsorbate is significantly larger than that obtained for the isoconcentration profiles of the eluent, and this occurs because the value of $(Pe_{intra})_a$ is about 21 times larger than the value of $(Pe_{intra})_e$. Additional results reported in Ref. [19] show that the magnitude of the departure from spherical symmetry of the isoconcentration profiles of the adsorbate and eluent increases as the magnitudes of $(Pe_{intra})_a$ and $(Pe_{intra})_e$ increase.

In Figs. 7 and 8, the dimensionless isoconcentration profiles of the adsorbate in the pore fluid of the pores of the macroporous region and in the adsorbed phase of the adsorbent particle are presented at three different times for $(Pe_{intra})_a = 10$ and $(Pe_{intra})_e = 0.476$, when case II is employed in the elution stage and the location of the adsorbent particles in the column is at $x = 0.2L$. The position in the column located at $x = 0.2L$ during the elution stage in case II corresponds to position $x = 0.8L$ during the adsorption stage; this means that at the beginning of the elution stage the concentration of the adsorbate in the adsorbed phase of the adsorbent particles located at $x = 0.2L$ is lower, in the system presented in Figs. 7 and 8, than the concentration of the adsorbate in the adsorbed phase of the adsorbent particles located at positions $x > 0.2L$. The outermost contours in Figs. 7 and 8 represent the isoconcentrations at the surface ($R = R_p$) of the particle. In Figs. 7 and 8, it can be observed that at $t_e = 0.1$ min there are isoconcentration contours that exhibit spherical asymmetry, as expected in particles with intraparticle convective flow (see Figs. 5 and 6 in

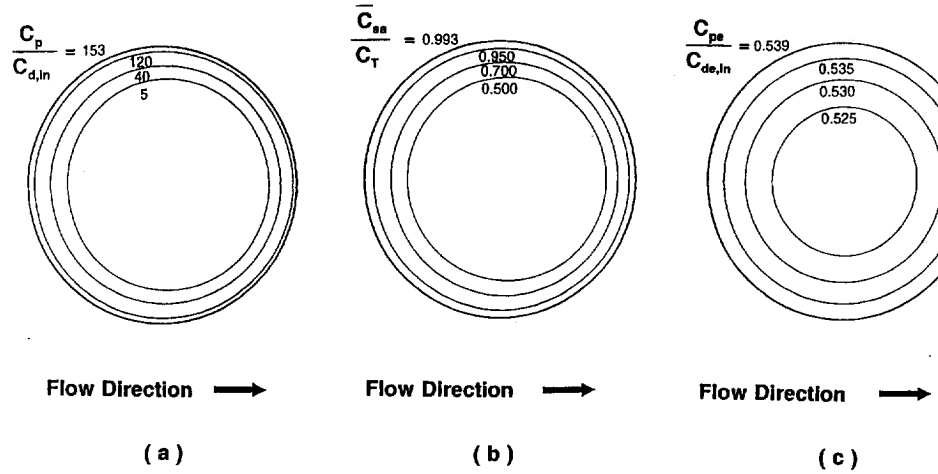

Fig. 5. Isoconcentration contours of the concentration of the adsorbate and eluent in the pore fluid of the macroporous region, and of the concentration of the adsorbate in the adsorbed phase of the porous adsorbent particle when case I is used with $(Pe_{intra})_a = 10$, $(Pe_{intra})_e = 0.476$ and $d_m = 7.00 \cdot 10^{-7}$ m, at $x = 0.2L$ and $t_e = 0.1$ min. (a) $C_p/C_{d,in}$; (b) $\bar{C}_{sa}/C_T$; (c) $C_{pe}/C_{de,in}$.

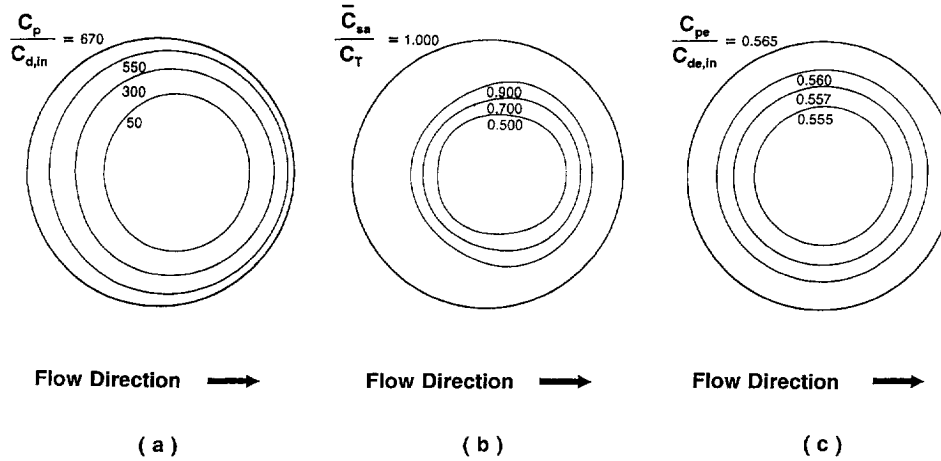

Fig. 6. Isoconcentration contours of the concentration of the adsorbate and eluent in the pore fluid of the macroporous region, and of the concentration of the adsorbate in the adsorbed phase of the porous adsorbent particle when case II is used with $(Pe_{intra})_a = 10$, $(Pe_{intra})_e = 0.476$ and $d_m = 7.00 \cdot 10^{-7}$ m, at $x = 0.8L$ and $t_c = 0.4$ min. (a) $C_p/C_{d,in}$; (b) $\bar{C}_{sa}/C_T$; (c) $C_{pe}/C_{de,in}$.

this paper and Refs. [8] and [9]), and certain isoconcentration contours located at intermediate positions in the particle have concentration values that are higher than those of the contours located at outer and inner parts of the particle; furthermore, there are, especially in the upstream region of the adsorbent particle, isoconcentration contours having very interesting geometrical shapes.

When the elution process starts, the eluent moves from the surface of the particle to the inner parts of the particle by intraparticle convective flow and diffusion and depending, for a given value of $t_e > 0$, on (i) the distribution of the penetration lengths of the eluent in the particle, with an eluent concentration greater than or equal to the critical eluent concentration along each length of the distribution of penetration lengths, and (ii) the values of the local rate of desorption of adsorbate at different positions

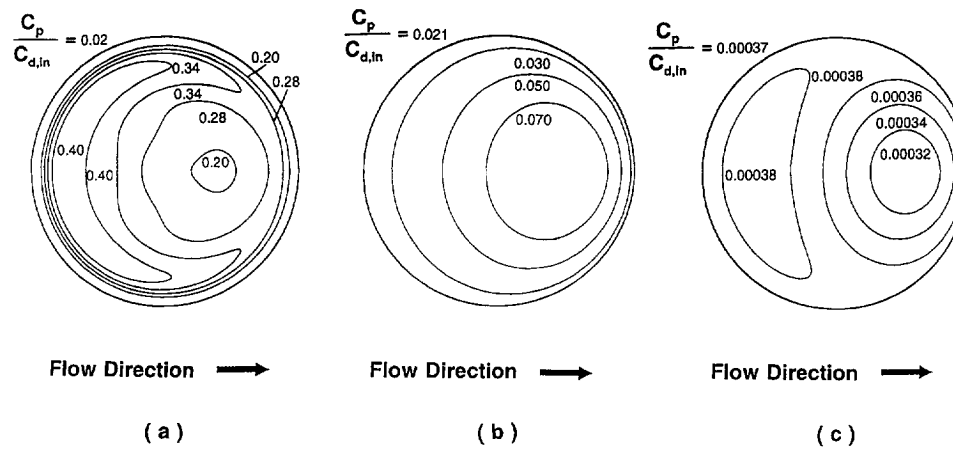

Fig. 7. Isoconcentration contours of the concentration of the adsorbate in the pore fluid of the macroporous region of the porous adsorbent particle for three different values of the elution time, t_e, when case II is used with $(Pe_{intra})_a = 10$, $(Pe_{intra})_e = 0.476$ and $d_m = 7.00 \cdot 10^{-7}$ m, at $x = 0.2L$. t_c = (a) 0.1, (b) 0.3 and (c) 0.4 min.

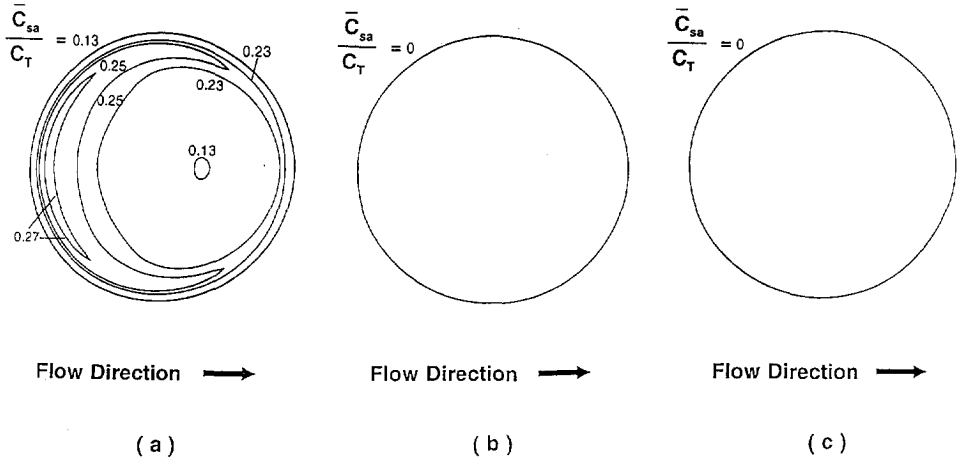

Fig. 8. Isoconcentration contours of the concentration of the adsorbate in the adsorbed phase of the porous adsorbent particle for three different values of the elution time, t_e, when case II is used with $(Pe_{intra})_a = 10$, $(Pe_{intra})_e = 0.476$ and $d_m = 7.00 \cdot 10^{-7}$ m, at $x = 0.2L$. t_e = (a) 0.1, (b) 0.3 and (c) 0.4 min.

along each penetration length of the eluent, isoconcentration contours could be obtained with geometries and distribution of concentration values at different parts of the particle as those shown in Figs. 7 and 8 at $t_e = 0.1$ min. As the elution time, t_e, becomes ≥ 0.3 min, it can be observed in Fig. 7 that the value of the concentration C_p has been reduced significantly everywhere in the particle. The results in Fig. 8 indicate that when $t_e \geq 0.3$ min the concentration of the adsorbate in the adsorbed phase is equal to zero everywhere in the particle, and this indicates that the eluent has completely desorbed the adsorbate from the surface of the pores of the macroporous and microporous regions of the particle.

Finally, model simulations using the values of the parameters in Tables 1 and 2, the values of the intraparticle Peclet numbers reported in the captions of Figs. 1–8, and considering the size of the microsphere to be either (a) $d_m = 7.00 \cdot 10^{-8}$ m or (b) $d_m = 7.00 \cdot 10^{-6}$ m, provided [19] elution peaks for the adsorbate, breakthrough curves for the eluent, and isoconcentration contours for the concentration of the adsorbate and eluent in the adsorbent particles, whose behavior was similar to the behavior of the results presented in Figs. 1–8.

4. Conclusion

A mathematical model that could be used to describe elution (non-selective elution) in columns with spherical bidisperse perfusive or spherical bidisperse purely diffusive adsorbent particles was constructed and presented. A numerical solution procedure was also developed [19] and used to solve the unsteady-state spatially multi-dimensional non-linear partial differential equations of the model. The numerical solution of the mathematical model allows the determination of (a) the intraparticle concentration profiles of the adsorbate in the pore fluid and in the adsorbed phase, (b) the intraparticle concentration profiles of the eluent in the pore fluid, (c) the transport rates of the adsorbate and eluent and the desorption rates of the adsorbate, for a variety of adsorbent particle characteristics and operating conditions in the column, and (d) the concentrations of the adsorbate and eluent in the flowing fluid stream everywhere in the column including its exit, for intraparticle Peclet numbers for the adsorbate and eluent ≥ 0.

The results of this work indicate that the spherical symmetry of the isoconcentration contours of the adsorbate during elution inside a purely diffusive [19] porous adsorbent particle

$[(Pe_{intra})_a = (Pe_{intra})_e = 0]$ is significantly altered as the values of $(Pe_{intra})_a$ and $(Pe_{intra})_e$ are increased (particles with intraparticle fluid flow). The isoconcentration contours of the concentrations of the adsorbate in the pore fluid and in the adsorbed phase exhibit spherical asymmetry during elution, when particles with intraparticle fluid flow are employed; the departure from spherical symmetry increases as $(Pe_{intra})_a$ and $(Pe_{intra})_e$ increase.

It was also found that as $(Pe_{intra})_a$ increases, the asymmetry of the elution peak of the adsorbate (at the exit of the column) decreases, the peak height increases and the time required for the elution of the adsorbate decreases. The results of this work also show that T_e decreases and $C_{d,bulk}$ and the concentration factor, CF, increase, as the diameter of the microsphere, d_m, decreases and the value of $(Pe_{intra})_a$ increases for the adsorbent particles used in the column. Finally, the results clearly show that for given values of d_m and $(Pe_{intra})_a$, the systems of case II (systems with reverse flow during the elution stage) exhibit better performance than that obtained from the systems of case I (same direction of flow during the adsorption and elution stages).

Symbols

C_d	concentration of adsorbate in the flowing fluid stream of the column, kg/m^3 of bulk fluid
$C_{d,bulk}$	average bulk concentration of the adsorbate defined in Eq. 34, kg/m^3 of bulk fluid
C_{de}	concentration of eluent in the flowing fluid stream of the column, kg/m^3 of bulk fluid
$C_{d,in}$	inlet concentration of adsorbate to the column during the adsorption stage, kg/m^3 of bulk fluid
$C_{de,in}$	concentration of eluent at $x < 0$ when $D_{Le} \neq 0$, or at $x = 0$ when $D_{Le} = 0$, kg/m^3 of bulk fluid
C_p	concentration of adsorbate in the fluid of the macropores, kg/m^3 of macropore volume
C_{pe}	concentration of eluent in the fluid of the macropores, kg/m^3 of macropore volume
C_{pm}	concentration of adsorbate in the fluid of the micropores, kg/m^3 of micropore volume
C_{pme}	concentration of eluent in the fluid of the micropores, kg/m^3 of micropore volume
$\bar{C}_{pme}$	average concentration of eluent, kg/m^3 of microparticle
$C_{pme,cr}$	critical eluent concentration, kg/m^3 of micropore volume
$\bar{C}_s$	average concentration of adsorbate, kg/m^3 of microparticle
$\bar{C}_{sa}$	average concentration of adsorbate in the adsorbed phase defined in Eq. 33, kg/m^3 of adsorbent particle
C_{sm}	concentration of adsorbate in the adsorbed phase of the microparticle, kg/m^3 of adsorbent particle
C_T	maximum equilibrium concentration of adsorbate in the adsorbed phase of the microparticle, kg/m^3 of adsorbent particle
CF	concentration factor defined in Eq. 35, dimensionless
d_p	diameter of spherical porous adsorbent particle ($d_p = 2R_p$), m
D_L	axial dispersion coefficient of adsorbate, m^2/s
D_{Le}	axial dispersion coefficient of eluent, m^2/s
d_m	diameter of spherical microparticle ($d_m = 2r_m$), m
D_p	effective pore diffusion coefficient of adsorbate in the macropores, m^2/s
D_{pe}	effective pore diffusion coefficient of eluent in the macropores, m^2/s
D_{pm}	effective pore diffusion coefficient of adsorbate in the micropores, m^2/s
D_{pme}	effective pore diffusion coefficient of eluent in the micropores, m^2/s
F	parameter given by Eq. 10 in Ref. [8]
H	parameter given by Eq. 11 in Ref. [8]
k_1	rate constant in Eq. 25, m^3 of micropore volume/kg · s
k_2	rate constant in Eq. 25, s^{-1}

k_3 rate constant in Eq. 26, s^{-1}
K equilibrium adsorption constant of adsorbate, $K = k_1/k_2$, m^3/kg
L column length, m
$(Pe_{intra})_a$ intraparticle Peclet number of adsorbate defined in Eq. 11, dimensionless
$(Pe_{intra})_e$ intraparticle Peclet number of eluent defined in Eq. 12, dimensionless
r radial distance in microparticle, m
r_m radius of microparticle, m
R radial distance in adsorbent particle, m
R_p radius of adsorbent particle, m
t_e time during the elution stage, s
T temperature, K
T_e total time of the duration of the elution stage, s
v_p intraparticle velocity vector, m/s
v_{pR} intraparticle velocity component along the R direction, m/s
$v_{p\theta}$ intraparticle velocity component along the θ direction, m/s
V_f column fluid superficial velocity, m/s
x axial distance in column, m

Greek letters

ε void fraction in column
ε_p macropore void fraction
ε_{pm} micropore void fraction
θ polar coordinate angle, rad

Acknowledgement

The authors gratefully acknowledge partial support of this work by Monsanto.

References

[1] B.H. Arve and A.I. Liapis, Biotechnol. Bioeng., 30 (1987) 638.
[2] A.I. Liapis, Sep. Purif. Methods, 19 (1990) 133.
[3] A.I. Liapis and M.A. McCoy, J. Chromatogr., 599 (1992) 87.
[4] M.A. McCoy, A.I. Liapis and K.K. Unger, J. Chromatogr., 644 (1993) 1.
[5] A.I. Liapis and M.A. McCoy, J. Chromatogr. A, 660 (1994) 85.
[6] A.I. Liapis, Math. Modelling Sci. Comput., 1 (1993) 397.
[7] A.I. Liapis and K.K. Unger, in G. Street (Editor), Highly Selective Separations in Biotechnology, Blackie, Glasgow, 1994, pp. 121–162.
[8] A.I. Liapis, Y. Xu, O.K. Crosser and A. Tongta, J. Chromatogr. A, 702 (1995) 45.
[9] G.A. Heeter and A.I. Liapis, J. Chromatogr. A, 711 (1995) 3.
[10] N.B. Afeyan, N.F. Gordon, I. Mazsaroff, L. Varady, S.P. Fulton, Y.B. Yang and F.E. Regnier, J. Chromatogr., 519 (1990) 1.
[11] B.H. Arve and A.I. Liapis, AIChE J., 33 (1987) 179.
[12] B.H. Arve and A.I. Liapis, in A.I. Liapis (Editor), Fundamentals of Adsorption, Engineering Foundation, distributed by the American Institute of Chemical Engineers, New York, 1987, pp. 73–87.
[13] F.H. Arnold, H.W. Blanch and C.R. Wilke, Chem. Eng. J., 30 (1985) B25.
[14] D.J. Gunn, Trans. Inst. Chem. Eng. (London), 49 (1971) 109.
[15] D.J. Gunn, Chem. Eng. Sci., 42 (1987) 363.
[16] F.H. Arnold, H.W. Blanch and C.R. Wilke, Chem. Eng. J., 30 (1985) B9.
[17] G. Carta and A.E. Rodrigues, Chem. Eng. Sci., 48 (1993) 3927.
[18] G. Neale, N. Epstein and W. Nader, Chem. Eng. Sci., 28 (1973) 1865.
[19] Y. Xu, Ph.D. Dissertation, University of Missouri–Rolla, 1995.